densed O_2 is present at the equatorial latitudes than at the colder poles[4]. The mechanism proposed here is applicable to electronic excitations caused by essentially any radiation source (electrons, ions or photons), provides a quantitative understanding of O_2 formation in ice, and indicates that oxygen is probably also produced on other icy outer Solar System bodies. □

Received 8 December 1997; accepted 27 April 1998.

1. Spencer, J. R., Calvin, W. M. & Person, M. J. Charge-coupled device spectra of the Galilean satellites: Molecular oxygen on Ganymede. *J. Geophys. Res.* **100,** 19049–19056 (1995).
2. Hall, D. T., Strobel, D. F., Feldman, P. D., McGrath, M. A. & Weaver, H. A. Detection of an oxygen atmosphere on Jupiter's moon Europa. *Nature* **373,** 677–679 (1995).
3. Calvin, W. M., Johnson, R. E. & Spencer, J. R. O_2 on Ganymede: Spectral characteristics and plasma formation mechanisms. *Geophys. Res. Lett.* **23,** 673–676 (1996).
4. Calvin, W. M. & Spencer, J. R. Latitudinal distribution of O_2 on Ganymede: Observations with the Hubble Space Telescope. *Icarus* **130,** 505–516 (1997).
5. Johnson, R. E. Sputtering of ices in the outer solar system. *Rev. Mod. Phys.* **68,** 305–312 (1996).
6. Johnson, R. E. & Quickenden, T. I. Photolysis and radiolysis of water ice on outer solar system bodies. *J. Geophys. Res.* **102,** 10985–10996 (1997).
7. Vidal, R. A., Bahr, D., Baragiola, R. A. & Peters, M. Oxygen on Ganymede: Laboratory studies. *Science* **276,** 1839–1842 (1997).
8. Ip, W.-H., Williams, D. J., McEntire, R. W. & Mauk, B. Energetic ion sputtering effects at Ganymede. *Geophys. Res. Lett.* **24,** 2631–2634 (1997).
9. Lanzerotti, L. J., Brown, W. L., Poate, J. M. & Augustyniak, W. M. On the contribution of water products from Galiliean satellites to the Jovian magnetosphere. *Geophys. Res. Lett.* **5,** 155–158 (1978).
10. Johnson, R. E. *Energetic Charged-particle Interactions with Atmospheres and Surfaces* (Springer, Berlin, 1990).
11. Johnson, R. E., Lanzerotti, L. J., Brown, W. L. & Armstrong, T. P. Erosion of Galilean satellite surfaces by Jovian magnetosphere particles. *Science* **212,** 1027–1030 (1980).
12. Brown, W. L., Lanzerotti, L. J., Poate, J. M. & Augustyniak, W. M. "Sputtering" of ice by MeV light ions. *Phys. Rev. Lett.* **40,** 1027–1030 (1978).
13. Kimmel, G. A. & Orlando, T. M. Low-energy (5-120 eV) electron-stimulated dissociation of amorphous D_2O ice: $D(^2S)$, $O(^3P_{2,1,0})$ and $O(^1D_2)$ yields and velocity distributions. *Phys. Rev. Lett.* **75,** 2606–2609 (1995).
14. Sieger, M. T., Simpson, W. C. & Orlando, T. M. Electron-stimulated desorption of D^+ from D_2O ice: Surface structure and electronic excitations. *Phys. Rev. B* **56,** 4925–4937 (1997).
15. Brown *et al.* Erosion and molecule formation in condensed gas films by electronic energy loss of fast ions. *Nucl. Inst. Methods* **198,** 1–8 (1982).
16. Reimann, C. T. *et al.* Ion-induced molecular ejection from D_2O ice. *Surf. Sci.* **147,** 227–240 (1984).
17. Westley, M. S., Baragiola, R. A., Johnson, R. E. & Baratta, G. A. Photodesorption from low-temperature water ice in interstellar and circumsolar grains. *Nature* **373,** 405–407 (1995).
18. Simpson, W. C. *et al.* Dissociative electron attachment in nanoscale ice films: Temperature and morphology effects. *J. Chem. Phys.* **107,** 8668–8678 (1997).
19. Bednarek, J., Plonka, A., Hallbrucker, A., Mayer, E. & Symons, M. C. R. Hydroperoxyl radical generation by gamma-irradiation of glassy water at 77 K. *J. Am. Chem. Soc.* **118,** 9387–9390 (1996).
20. Taub, I. A. & Eiben, K. Transient solvated electron, hydroxyl, and hydroperoxy radicals in pulse-irradiated crystalline ice. *J. Chem. Phys.* **49,** 2499–2513 (1968).
21. Noll, K. S., Johnson, R. E., McGrath, M. A. & Caldwell, J. J. Detection of SO_2 on Callisto with the Hubble Space Telescope. *Geophys. Res. Lett.* **24,** 1139–1142 (1997).
22. Noll, K. S., Johnson, R. E., Lane, A. L., Domingue, D. L. & Weaver, H. A. Detection of ozone on Ganymede. *Science* **273,** 341–343 (1996).
23. Lacombe, S. *et al.* Electron-induced synthesis of ozone in a dioxygen matrix. *Phys. Rev. Lett.* **79,** 1146–1149 (1997).

Acknowledgements. We thank G. A. Kimmel for discussions. This work was supported by the US Department of Energy, Office of Basic Energy Sciences, Chemical Physics Program. Pacific Northwest National Laboratory is operated for the US Department of Energy by Battelle Memorial Institute.

Correspondence and requests for materials should be addressed to T.M.O. (e-mail: tm_orlando@pnl. gov).

Fluctuation-induced diffusive instabilities

David A. Kessler* & Herbert Levine†

* *Minerva Center and Department of Physics, Bar-Ilan University, Ramat Gan, Israel*

† *Department of Physics, University of California, San Diego, La Jolla, California 92093-0319, USA*

The formation of complex patterns in many non-equilibrium systems, ranging from solidifying alloys to multiphase flow[1], nonlinear chemical reactions[2] and the growth of bacterial colonies[3,4], involves the propagation of an interface that is unstable to diffusive motion. Most existing theoretical treatments of diffusive instabilities are based on mean-field approaches, such as the use of reaction–diffusion equations, that neglect the role of fluctuations. Here we show that finite fluctuations in particle number can be essential for such an instability to occur. We study, both analytically and with computer simulations, the planar interface separating different species in the simple two-component reaction A + B → 2A (which can also serve as a simple model of bacterial growth in the presence of a nutrient). The interface displays markedly different dynamics within the reaction–diffusion treatment from that when fluctuations are taken into account. Our findings suggest that fluctuations can provide a new and general pattern-forming mechanism in non-equilibrium growth.

We consider a slightly modified version[5] of an "infection" model due to Blumen *et al.*[6,7]. There are two types of particles, infectious (A) and non-infected but susceptible (B). Both particle types move diffusively on a lattice, with no constraint on multiple occupancy, with differing rates D_A and D_B. A B particle which is co-located with an A particle has some probability per unit time of becoming infected, that is, changing to an A. At the mean-field level in which we ignore particle number fluctuations, the dynamics of this system is describable via the coupled reaction–diffusion equations:

$$\frac{\partial c_A}{\partial t} = \nabla^2 c_A + c_A c_B$$
$$\frac{\partial c_B}{\partial t} = D\nabla^2 c_B - c_A c_B \qquad (1)$$

Here we have scaled out the reaction rate and furthermore scaled space so as to eliminate D_A in the first equation; D is defined as the ratio D_B/D_A. Formally, this equation can be obtained as the limit of the underlying Markov process when the average number of particles per site, N, goes to infinity. In the special case $D = 1$, this system reduces to the Fisher equation[8].

Our interest here is in interface propagation, namely the process whereby introduction of some number of A particles at the left edge of a finite region filled with B particles at some initial concentration c_B^0 leads to the development of a moving front. The velocity of such a front in the reaction–diffusion approximation follows from the marginal stability principle[9–11]:

$$v_{MS} = 2\sqrt{c_B^0} \qquad (2)$$

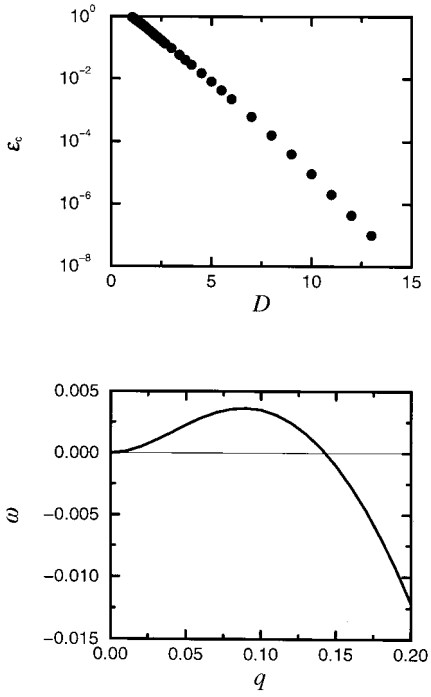

Figure 1 Results of stability analysis. Top, dependence of the critical value ϵ_c of the cut-off as a function of the diffusion-constant ratio D. Bottom, spectrum at $D = 10$, $\epsilon = 0.0014$. See Methods for details.

In what follows we take $c_B^0 = 1$ without loss of generality. It has recently been established[5,12] that, in models such as this one, the difference between the velocity of the microscopic process and that predicted by the above analysis exhibits the characteristic scaling form $v_{MS} - v(N) \sim 1/\log^2 N$. For example, a direct demonstration of this for the $D = 1$ case was recently presented in Kessler *et al.*[5] Brunet and Derrida[12] have argued that this specific form can be understood as arising from an effective cut-off which needs to be placed into the continuum description, a cut-off arising from discrete particle number effects. This cut-off limits the reaction term to values of the A concentration greater than some small number $\epsilon \approx 1/N$, and leads to the above result, independent of the exact form of the cut-off. We note that similar ideas had been proposed earlier, in the contexts of diffusion-limited aggregation[13] and RNA virus evolution[14], although a derivation of this deterministic cut-off approach (including for example, the exact correspondence between ϵ and N) from the master equation for the stochastic process is still lacking.

Although the velocity shift just described is quantitatively significant, the cut-off effect does not alter the qualitative form of the interface in a one-dimensional system. This changes dramatically when we go to higher dimensions. To show this, we focus on the stability of a planar interface in the modified continuum model obtained by setting the reaction term to zero if c_A is below ϵ. The steady-state profile as a function of D and ϵ is determined numerically, and the linear stability operator is defined in standard fashion by expanding the basic equations around this solution in the moving frame of reference. Because of translation invariance in the transverse directions, modes of this operator can be labelled by a transverse wavevector $\mathbf{q}$ and the growth rate ω is a function of the magnitude, q, of this vector. As the mode with $\mathbf{q} = 0$ is merely a translation of the entire front, this must have growth rate zero.

Performing this calculation, we find that for a given diffusion ratio D, there is a critical value of the cut-off, ϵ_c, such that the interface is unstable for all $\epsilon > \epsilon_c$. In Fig. 1a, we show a graph of ϵ_c as a function of D. Equivalently, we may view the graph as showing the minimum value of D for which there is an instability at a given ϵ. We see from the graph that this minimum D diverges as $\epsilon \to 0$ as $\ln(1/\epsilon)$. This behaviour can be understood as follows. Diffusive instabilities require that the scale of the diffusing field D/v be sufficiently large compared to the width of the (linearly unstable) reaction zone. Here, the only thing limiting the spread of this zone is the finite cut-off. For small ϵ, this width scales as $\log(1/\epsilon)$; this was shown explicitly in Brunet and Derrida[12] for the cut-off Fisher equation and is easily extended to the present case. This explains why, in the absence of a cut-off, the interface is stable for all D. Thus we find that the naive reaction–diffusion approach misses the entire possibility that the interface can be unstable.

In Fig. 1b, we plot the full spectrum for a typical case ($D = 10$, $\epsilon = 0.0014$) inside the unstable region. We find that the instability begins at $q = 0$ and extends to some finite q. This type of spectrum with its long wavelength instability is directly indicative of the diffusive nature of the instability; one could compare this graph to the Mullins–Sekerka[15] spectrum for alloy solidification, to take one example. In Fig. 2, we show results from a simulation of the cut-off reaction–diffusion system (for a different parameter set), showing the growth of initially small perturbations to the planar interface. Our theory predicts, therefore, that the non-equilibrium dynamics of our microscopic model exhibits a pattern-forming mechanism that is completely missed by the standard treatment. To verify this, we have performed a direct simulation of a two-dimensional system. We present in Fig. 3 the results of three computations, providing unambiguous evidence that this is indeed the case. The interface with $D = 10$ and $N = 1{,}000$ is diffusively unstable, as it supports large cellular structures with grooves where growth is screened out. Going to large N at fixed D eliminates the instability, as predicted by the analytic treatment. Finally, if we set $D = 1$ and $N = 1{,}000$, the interface is again stable as predicted, but now shows significant fluctuations, as expected from the work of Kardar, Parisi and Zhang[16].

One application of these ideas is to a series of experiments on unstable interfaces which arise during the nutrient-limited growth of bacterial colonies on agar[3,4,17]. The simplest model of such a process would contain (rapidly diffusing) nutrient particles (B) which are devoured by (slowly-diffusing) bacteria (A), thereby allowing the latter to reproduce. This model is very similar to Blumen kinetics, and can be expected to have exactly the same instability if one takes into account the cut-off effect; without the cut-off it is always stable (E. Ben-Jacob and I. Cohen, personal

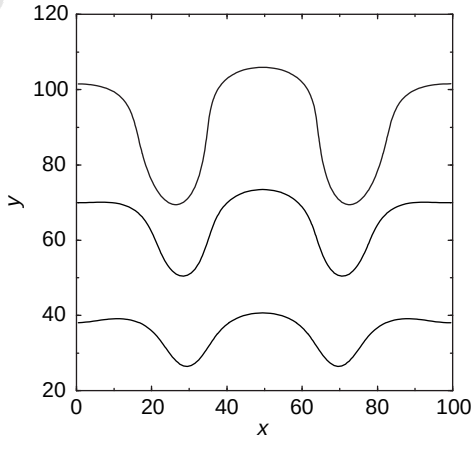

Figure 2 Results of a simulation of the reaction–diffusion equations with $D = 10$ and $\epsilon = 0.25$. The equations are discretized on a grid of size 100×200, with lattice spacing one and periodic boundary conditions in x. The fields are updated using explicit time steps of $\Delta t = 0.01$. The lines shown in the graph are the $c_A = 0.75$ contour lines for three different times, separated by 150 units. The graph depicts a region of size 40×100 which spans the interface; the three different lines have been translated in y so as to better depict the shape change.

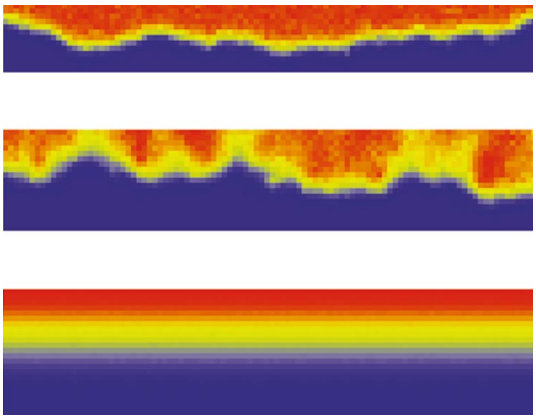

Figure 3 Results of a simulation of the microscopic reaction model. The cases shown are the cases $D = 10$ (top) and $D = 1$ (middle), both for $N = 1{,}000$ and a reaction rate constant $k = 10^{-4}$; and $D = 10$, $N = 10^4$ with $k = 10^{-5}$ (bottom). The graph shows the interfacial region for a box of width 100; the colour scale corresponds to the number of A particles (red is $N_A \simeq N$, blue is $N_A \simeq 0$). Each site of a 100×200 lattice has some number of A and B particles. Initially, A particles are introduced at one edge, whereas B particles exist everywhere, with an average density of N. In each time step, particles can diffuse and same-site particles can react. The data shown is a typical snapshot of the interface once a statistical steady-state has been established.

communication). It is not yet clear whether this idea can quantitatively account for the instability, or whether a more complex model (possibly incorporating nonlinear diffusion[18]), which can give rise to instabilities even at the mean-field level, is more appropriate.

From the perspective of the general study of non-equilibrium physics, our finding are quite unusual. The fact that inevitable fluctuation effects in a finite density process can lead to such a drastic change in its large-scale properties is unexpected. This result complicates any attempt to use the calculational machinery of equilibrium statistical mechanics to study these systems, as these methods start from the point of view that fluctuation effects (in the form of additive thermal noise) become important only near a critical point. Here (and in the related process of diffusion-limited aggregation[19]), the fluctuations are due to discreteness (that is, they are shot-noise-like), enter multiplicatively and can be important even far from any critical scaling region. Our results indicate that a more sophisticated methodology which can account for the zeroth-order relevance of discreteness is a necessary starting point for analysing a wide class of interesting and important dynamical processes. □

Methods

The steady-state equation is

$$0 = vc'_A + c''_A + c_A c_B$$

$$0 = vc'_B + Dc''_B - c_A c_B$$

with $c_A(\infty) = 0$, $c_B(\infty) = 1$ and $'$ means d/dx in the moving frame. If we denote by x_ϵ the position at which $c_A = \epsilon$, we find (by matching to the region $x > x_\epsilon$);

$$c_A(x_\epsilon) = \epsilon \qquad c'_A(x_\epsilon) = -\epsilon v$$

$$c_B(x_\epsilon) = 1 - \delta_1 \qquad c'_B(x_\epsilon) = \delta_1 v/D$$

where δ_1 is as yet unknown. At large negative x, the most general asymptotic behaviour is;

$$c_A(x) \approx 1 + \delta_2 - \delta_3 e^{kx}$$

$$c_B(x) \approx \delta_3(vk + k^2)e^{kx}$$

with $k = -v/2D + [(v/2D)^2 + (1/D)]^{1/2}$. We integrate from both directions to $x = 0$ and impose $c_A(0) = 0.5$ so as to fix the translation invariance. These two conditions plus three continuity equations suffice to determine the five unknowns x_ϵ, v and the δs. In fact, δ_2 should be exactly zero due to a global conservation equation, and this can be used as a check on the accuracy of the numerical integration.

Once the steady-state is determined, we use a similar procedure for the stability spectrum. The equations we solve are, for $x < x_\epsilon$;

$$(\omega + q^2)\psi_A = v\psi'_A + \psi''_A + \psi_A c_B^{(0)} + \psi_B c_A^{(0)}$$

$$(\omega + Dq^2)\psi_B = v\psi'_B + D\psi''_B - \psi_A c_B^{(0)} - \psi_B c_A^{(0)}$$

where $c_{A,B} = c_{A,B}^{(0)} + \psi_{A,B}\exp(i\mathbf{q}\cdot y + \omega t)$. At large negative x, the asymptotic behaviour of the most general allowed solution for $\mathrm{Re}\,\omega > 0$ consists of;

$$\psi_A(x) \approx A_1\epsilon^{k_1 x} + A_2\epsilon^{k_2 x}$$

$$\psi_B(x) \approx -A_1(vk_1 + k_1^2 - q^2 - \omega)e^{k_1 x}$$

where

$$k_1 = -\frac{v}{2D} + \sqrt{\left(\frac{v}{2D}\right)^2 + \frac{1 + \omega + Dq^2}{D}}$$

$$k_2 = -\frac{v}{2} + \sqrt{\left(\frac{v}{2}\right)^2 + \omega + q^2}$$

The situation at x_ϵ needs to be handled carefully, as one must account for the fact that the perturbation in c_A will in general shift the position at which the cut-off sets in. This leads to the boundary conditions;

$$\psi_A(x_\epsilon) = A_4 \qquad \psi'_A(x_\epsilon) = A_4(k_4 + c_B^{(0)}(x_\epsilon)/v)$$

$$\psi_B(x_\epsilon) = A_3 \qquad \psi'_B(x_\epsilon) = A_3 k_3 - A_4 c_B^{(0)}(x_\epsilon)/Dv$$

where now

$$k_3 = -\frac{v}{2D} - \sqrt{\left(\frac{v}{2D}\right)^2 + \frac{\omega + Dq^2}{D}}$$

$$k_4 = -\frac{v}{2} - \sqrt{\left(\frac{v}{2}\right)^2 + \omega + q^2}$$

Imposing continuity conditions at $x = 0$ leads to a set of four homogeneous linear equation for the four As. The vanishing of the determinant of this system then determines the eigenvalue ω. This last step is implemented by a standard nonlinear equation solver. As a check on the accuracy of our procedure, we can solve for $\omega(q = 0)$ which should be precisely zero as it is just the translation mode. This number is typically of the order of 10^{-6} for our calculations.

Received 12 March; accepted 18 May 1998.

1. Kessler, D., Koplik, J. & Levine, H. Pattern selection in fingered growth phenomena. *Adv. Phys.* **37,** 255–339 (1988).
2. Horvath, D. & Toth, A. Diffusion-driven front instabilities in the chlorite-tetrathionate reaction. *J. Chem. Phys.* **108,** 1447–1451 (1998).
3. Matsushita, M. & Fujikawa, H. H. Diffusion-limited growth in bacterial colony formation. *Physica A* **168,** 498–506 (1990).
4. Ben-Jacob, E. *et al.* Generic modelling of cooperative growth patterns in bacterial colonies. *Nature* **368,** 46–49 (1994).
5. Kessler, D., Ner, Z. & Sander, L. M. Front propagation: precursors, cutoffs and structural stability. *Phys. Rev. E* **58,** 107–114 (1998).
6. Mai, J., Sokolov, I. M. & Blumen, A. Front propagation and local ordering in one-dimensional irreversible autocatalytic reactions. *Phys. Rev. Lett.* **77,** 4462–4465 (1996).
7. Mai, J., Sokolov, I. M., Kuzovkov, V. N. & Blumen, A. Front form and velocity in a one-dimensional autocatalytic A+B to 2A reaction. *Phys. Rev. E* **56,** 4130–4134 (1997).
8. Fisher, R. A. The wave of advance of advantageous genes. *Ann. Eugen.* **7,** 355–369 (1937).
9. Ben-Jacob, E., Brand, H., Dee, G., Kramer, L. & Langer, J. S. Pattern propagation in nonlinear dissipative systems. *Physica D* **14,** 348–364 (1985).
10. van Saarloos, W. Dynamical velocity selection: marginal stability. *Phys. Rev. Lett.* **58,** 2571–2574 (1987).
11. Paquette, G. C., Chen, L.-Y., Goldenfeld, N. & Oono, Y. Structural stability and renormalization group for propagating fronts. *Phys. Rev. Lett.* **72,** 76–79 (1994).
12. Brunet, E. & Derrida, B. Shift in the velocity of a front due to a cutoff. *Phys. Rev. E* **65,** 2597–2604 (1997).
13. Brener, E., Levine, H. & Tu, Y. Mean-field theory for diffusion-limited aggregation in low dimensions. *Phys. Rev. Lett.* **66,** 1978–1981 (1991).
14. Tsimring, L. S., Levine, H. & Kessler, D. A. RNA virus evolution via a fitness-space model. *Phys. Rev. Lett.* **76,** 4440–4443 (1996).
15. Mullins, W. W. & Sekerka, R. F. Stability of a planar interface during solidification of a dilute binary alloy. *J. Appl. Phys.* **35,** 444–451 (1964).
16. Kardar, M., Parisi, G. & Zhang, Y. C. Dynamic scaling of growing interfaces. *Phys. Rev. Lett.* **56,** 889–892 (1986).
17. Ben-Jacob, E. *et al.* Response of bacterial colonies to imposed anisotropy. *Phys. Rev. E* **53,** 1835–1843 (1996).
18. Newman, W. I. The long-time behavior of solutions to a nonlinear diffusion problem in population dynamics and combustion. *J. Theor. Biol.* **104,** 473–484 (1983).
19. Witten, T. A. & Sander, L. M. Diffusion-limited aggregation, a kinetic critical phenomenon. *Phys. Rev. Lett.* **47,** 1400–1403 (1981).

Acknowledgements. We thank L. Sander for discussions.

Correspondence and requests for materials should be addressed to H.L. (e-mail: hlevine@ucsd.edu).

Time-reversal symmetry-breaking superconductivity in Sr_2RuO_4

G. M. Luke*, Y. Fudamoto*, K. M. Kojima*, M. I. Larkin*, J. Merrin*, B. Nachumi*, Y. J. Uemura*, Y. Maeno†, Z. Q. Mao†, Y. Mori†, H. Nakamura‡ & M. Sigrist§

* *Department of Physics, Columbia University, New York, New York 10027, USA*
† *Department of Physics and* § *Yukawa Institute for Theoretical Physics, Kyoto University, Kyoto 606-8502, Japan*
‡ *Department of Material Science and Engineering, Kyoto University, Kyoto 606-8501, Japan*

Although the properties of most superconducting materials are well described by the theory[1] of Bardeen, Cooper and Schrieffer (BCS), considerable effort has been devoted to the search for exotic superconducting systems in which BCS theory does not apply. The transition to the superconducting state in conventional BCS superconductors involves the breaking of gauge symmetry